A MULTIFREQUENCY FM-BASED ULTRASONIC SYSTEM FOR ACCURACY 3D MEASUREMENT

F. Aldawi[1] , A. P. Longstaff[2], S. Fletcher[3], P. Mather[4], A. Myers[5] and J. Briggs[6]
University of Huddersfield, Queensgate, Huddersfield HD1 3DH, UK

ABSTRACT

This paper introduces an ultrasonic 3D position measurement system that will estimate the location of a wave source by triangulating its position based on a multiple-frequency continuous wave (MFcw) to three receivers fixed to an inertial frame of reference. The typical application of this system is finding the location of the transmitter that may be fixed on a CNC machine or robot. The receivers have to be fixed in specific locations, the major source of the problems are at the installation/calibration stage since the receivers are usually distributed in space and finding their exact location entails using a separate 3D calibrating device which may not be as accurate as the location system itself. This paper presents a method to use the system itself to set up an inertial frame of reference and find out the locations of the receivers.

Keywords Ultrasonic; 3D position measurement.

1 INTRODUCTION

There is a high demand for 3D ranging systems featuring high accuracy and extended range of operation. The possible applications are numerous and include position feedback for advanced control algorithms for 3D measurement systems in space. High accuracy 3D position measurement systems have typically been dominated by optical methods at a high associated cost. A one-dimensional ultrasonic measurement system using transmitter-receiver pair has been presented. The techniques of distance measurement using ultrasound in air includes the time-of-flight (TOF) technique' (Marioli (1992) and Tardajos et al (1994)), binary frequency-shift-keying (BFSK)' (Huang et al (2002)), binary amplitude-shift-keyed (BASK)' (Yang et al (2003)), and pulse compression' (Scheinzer et al (2005)). In time-of-flight method it is difficult to measure an accurate time of travel between transmitter and receiver.

BFSK method is more accurate than TOF method but still has a problem with measuring accurate time of travel between transmitter and receiver, this method and binary amplitude-shift-keyed method needed special hardware. The pulse compression method is based on transmitting a signal of several periods modulated in the frequency, the method is able to detect received signal with a resolution typically less than 1μs resulting in a distance resolution of about 0.17mm.

In order to obtain accurate distance estimation with low cost, the superior system choice is the phase data of a steady-state frequency received signal with reference to its transmitted signal. This is because the distance information is derived from the phase difference of a repeating signal which is sampled for statistically significant amounts of wave periods. Thus, the random variations in phase shift (from turbulence, environmental noise, electronic noise, etc.) tend to cancel themselves out in an averaging process. In most applications of range measurement in air using ultrasound, a phase-shift analysis of signal-frequency continuous-wave transmission is used to reduce error' (Huang et al (1998)). An extension of these techniques to 3D essentially involves a triangulation operation. In general, high accuracy ultrasonic systems currently available are limited by a compromise between accuracy and operating range. The literature on 3D ultrasonic position measurement systems is very scarce. This paper presents a 3D ultrasonic position measurement system implemented in prototype consisting of one transmitter mounted at the target point, and three receivers fixed in an inertial reference frame. A multiple-frequency continuous wave (MFcw) method with frequency modulation has been developed in this paper to obtain high accuracy for distance measurement, between transmitter and receivers, with consideration of change in temperature and humidity. The main advantage in this system is self-calibration, this is extremely important as it has a direct consequence on the accuracy of the system since the triangulation scheme uses the known positions of the transmitter to estimate the position of the receivers.

2 DISTANCE CALCULATION BY MFCW

The transmitted waveform and the received waveform in ultrasound are given at time t

$$Pi(t) = Ai \sin(\omega t) \tag{1}$$

$$\Pr(t) = Ar \sin(\omega t - \frac{2d(t)\omega}{c}) \tag{2}$$

Where Ai amplitude for transmitter signal, Ar amplitude for receiver signal, ω is the angular frequency of the waveform, *c* is the speed of sound, 2*d(t)* is the distance between ultrasound transmitter and receiver, thus, the phase delay between the transmitted and the received waveforms is given by

$\theta(t) = (\frac{2\pi}{\lambda}) \times 2d(t)$, and the formula can be written as

$$d(t) = \frac{\theta(t)}{2\pi} \times \frac{\lambda}{2} \tag{3}$$

Where λ *is the wavelength*, $\theta(t)$ is the phase shift and its value usually cycles between zero to *2π.* The moving distance, $d(t)$, can be uniquely determined by the phase shift $\theta(t)$ and the maximum ranging distance does not exceed the half wavelength for absolute distance measurement. If the maximum ranging distance exceeded the half wavelength, a phase ambiguity occurs. In other words, the measured moving distance is limited to half wavelength. For instance, λ is approximately 3.5m when a 100 Hz signal is used. When the distance between the transmitter and the receiver is more than 1.75m, the value of $\theta(t)$ varies around 2π . Such a small maximum range greatly limits the use of phase detection methods to measure moving distance. To overcome this limitation, a method to count the integer number of wavelength occurring as the measured displacement increases is used. The total displacement $d(t)$ is determined by the formula,

$$d(t) = n \times \lambda + \frac{\theta(t)}{2\pi} \times \frac{\lambda}{2} \tag{4}$$

Where n is the number of the wavelength. Three different ultrasound signal frequencies, f_1, f_2 and f_3 are used in this research to measurement the total displacement $d(t)$, where $f_1 < f_2 < f_3$ The phase shift θ_1 of the f_1 signal with the longest wavelength λ_1 , gives the first approximation of displacement $d_1(t)$ if the movement of the object dose not exceed half wavelength.

$$d(t) = d_1(t) = \frac{\theta_1(t)}{2\pi} \times \frac{\lambda_1}{2} \tag{5}$$

Using a higher frequency f_2 signal to measure the same range with a finer ranging resolution causes a greater phase shift than frequency f_1 signal due to the small change in the pathlength. The integer number N_2 of wavelength of frequency f_2 signal can be calculated from

$$N_2 = Int[\frac{d_1(t)}{\lambda_2}].$$

The second approximation to the displacement $d(t)$ is obtained from the phase shift θ_2 of frequency f_2 signal, the number N_2 of the wavelength λ_2 , as described in the following equation:

$d(t) = N_2 \times \lambda_2 + d_2(t)$, where $d_2(t) = \frac{\theta_2(t)}{2\pi} \times \frac{\lambda_2}{2}$,

Similarly, the phase shift θ_3 of frequency f_3 signal, and

$$N3 = Int[\frac{d_2(t)}{\lambda 3}].$$

$$d(t) = N_2 \times \lambda_2 + N_3 \times \lambda_3 + d_3(t)$$

Where:

$$d3(t) = \frac{\theta_3(t)}{2\pi} \times \frac{\lambda 3}{2} \tag{6}$$

The final equation concluded from the above equations is shown as follows,

$$d(t) = Int[\frac{d_1(t)}{\lambda_2}] \times \frac{\lambda_2}{2} + Int[\frac{d_2(t)}{\lambda_3}] \times \frac{\lambda_3}{2} + \frac{\theta_3(t)}{2\pi} \times \frac{\lambda_3}{2}$$

Substituting $d_1(t)$ and $d_2(t)$

$$d(t) = Int[\frac{\theta_1(t)}{4\pi} \times \frac{\lambda 1}{\lambda 2}] \times \frac{\lambda 2}{2} + Int[\frac{\theta 2(t)}{4\pi} \times \frac{\lambda 2}{\lambda 3}] \times \frac{\lambda 3}{2} + \frac{\theta 3(t)}{2\pi} \times \frac{\lambda 3}{2}$$

$$d(t) = Int[\frac{\theta_1(t)}{4\pi} \times \frac{f_2}{f_1}] \times \frac{c}{2f_2} + Int[\frac{\theta_2(t)}{4\pi} \times \frac{f_3}{f_2}] \times \frac{c}{2f_3} + \frac{\theta 3(t)}{4\pi} \times \frac{c}{f_3} \tag{7}$$

Where *c* is the current value of the speed of sound. The maximum distance and minimum resolution that can be achieved are determined by the choice of frequencies f_1, f_2 and f_3. In order to be able to measure large displacement, $f_1 = 100$ *Hz*, $f_2 = 1$ *KHz and* $f_3 = 40$ *KHz.*

Most commercial ultrasound transducers are fabricated on the principle of frequency resonance for achieving a high sensitivity at lower operating frequencies *(40 ± 2 kHz),* which results in narrow-bandwidth devices. Fortunately, MFcw can achieve a narrow bandwidth ultrasound ranging system.

3 TEMPERATURE CALCULATION

Substituting the equation of state of air of an ideal gas *(PV = RT)* and the definition of density ρ (mass per unit volume), the speed of sound in air may be rewritten as

$$c = \sqrt{\frac{1.4RT}{M}} \tag{8}$$

Where *R* is the universal gas constant *(R= 8.315410 J. mol^{-1}. K^{-1})* , *T* the absolute temperature in Kelvins, and *M* the mean molecular weight of gas at sea level.
T = t + 273.15, Where t is the temperature in degrees Celsius.

$$c = 331.3\sqrt{1 + \frac{t}{273.15}} \tag{9}$$

Eq. (7), May be rewritten as

$$d(t) = (Int[\frac{\theta_1(t)}{4\pi} \times \frac{f_2}{f_1}] \times (331.3\sqrt{1+\frac{t}{273.15}}) \times \frac{1}{2f_2}) + (Int[\frac{\theta_2(t)}{4\pi} \times \frac{f_3}{f_2}] \times (331.3\sqrt{1+\frac{t}{273.15}}) \times \frac{1}{2f_3}) + (\frac{\theta_3(t)}{4\pi} \times (331.3\sqrt{1+\frac{t}{273.15}}) \times \frac{1}{f_3}) \tag{10}$$

4 HUMIDITY CALCULATION

All previous discussion assumed dry air. Attention turns now to the effects of moisture on the speed of sound. Moisture affects the density of air hence, the specific –heat ratio and molecular weight can now be rewritten to include the effects of moisture for air as

$$\mu\omega = \frac{7+h}{5+h} \tag{11}$$

$$M\omega = 29 - 11h \tag{12}$$

Eqs. (11) And (12) modify the two terms from Eq. (8) affected by the addition of water vapour to air. Both are a function of the introduced water molecule fraction *h*. Relative humidity *RH* (expressed as a percentage) is defined such that

$$h = \frac{0.01 \times RH \times e(t)}{P} \tag{13}$$

Where *P* equals ambient pressure *(1.013 * 10^5 Pa)* and *e(t)* is the vapour pressure of water at temperature t. Eq. (10), can now be rewritten include the effects of moisture also for as

$$d(t) = (Int[\frac{\theta_1(t)}{4\pi} \times \frac{f2}{f1}] \times (\sqrt{\frac{\mu\omega \times R \times T}{M\omega}}) \times \frac{1}{2f2}) + (Int[\frac{\theta 2(t)}{4\pi} \times \frac{f_3}{f_2}] \times (\sqrt{\frac{\mu\omega \times R \times T}{M\omega}}) \times \frac{1}{2f3}) + (\frac{\theta 3(t)}{4\pi} \times (\sqrt{\frac{\mu\omega \times R \times T}{W\omega}}) \times \frac{1}{f3}) \tag{14}$$

5 DETERMINATION OF THE COORDINATES OF WAVE SOURCE

This mode is used to find the coordinates of the transmitter (source) with respect to the inertial frame of reference of the fixed receivers. The minimum number of receivers required to obtain a solution is three, but more may be used for higher accuracy.
The distances between the transmitter and the receivers are measured by MScw method. A new algorithm for 3D positions has been developed during this paper to allow the receivers to be located arbitrarily at convenient positions. This is important for efficient implements on a machine.
By consider the following case in Figure. 1 where 3 receivers, R_1, R_2 and R_3 are employed:
The coordinate of the position $p(x, y, z)$ can be simply obtained by multiplying the rotation matrices (α, β and θ angles on the corresponding axis x, y and z) with an inverse transformation matrix, which is derived as follows:

$$\begin{bmatrix} x \\ y \\ z \\ 1 \end{bmatrix} = \left[Rot(x,\theta).Rot(y,\beta).Rot(z,\alpha).Tran(x_1, y_1, z_1)\right]^{-1}.\begin{bmatrix} x' \\ y' \\ z' \\ 1 \end{bmatrix} \tag{15}$$

6 RECEIVER'S SELF-CALIBRATION

The receivers' positions are established in an *xyz* coordinate system ***R,*** Shown as follows (Figure. 2):
Where, receiver 1 is assumed to be at the origin (0, 0, 0) and receiver 2 is on the x-axis, represented as $R_2(x_2, 0, 0)$, thus x_2 equals the distance between receiver 1 and receiver 2, a, that can be measured using the multiple-frequency continuous wave (MFcw) by configuring receiver 2 as the transmitter.

$$x_2 = a \tag{16}$$

Here the z-axis is assumed to be orthogonal with the plane $R_1 R_2 R_3$, which is determined by the three receivers. Thus, receiver 3 has the coordinate $(x_3, y_3, 0)$ that can be determined with:

$x_3 = b.\cos\alpha$, Then, substituting,

$\cos\alpha = \dfrac{a^2 + b^2 - c^2}{2ab}$, Yields:

$$x_3 = \frac{a^2 + b^2 - c^2}{2a} \tag{17}$$

Where *b, c* are also measured by multiple-frequency continuous wave (MFcw) system with the receiver 3 configured as transmitter. Once x_3 is determined, y_3 can then be calculated with the following equation:

$$y_3 = \sqrt{b^2 - x_3^2} \tag{18}$$

7 EXPERIMENTAL RESULTS

As shown in the block diagram of Figure. 3 the system consists of four ultrasound transducers (one of them is used to transmit the signal and three are used to receive the signal), auto-gain-controlled amplifier system, DAQ (one output used as transmit the signal, three input used as receive the signal), temperature and humidity sensors (using ultrasonic sensors°), and a microprocessor used to govern the operation of the entire system.
LABVIEW software is used to generate a stable frequency sine wave, generating three frequencies 100Hz and 1 kHz, 40 KHz and then applying them to frequency modulation (FM) by using 40 KHz as

carrier. The carrier frequency was selected, because the transducers used have a frequency bandwidth with a centre frequency at 40kHz±2.
The system must be calibrated by operating it at a known distance at frequencies 40 kHz, 1 kHz and 100 Hz. The CMM machine is used to calibrate the system at temperatures changing from 26.19Cº to 26.85Cº. The temperature and humidity measured by ultrasonic system to reduce the error produced from effect of temperature on speed of sound.
Figure. 4 shows the different phase between the signals from transmitter to receiver, figure. 5 shows the operation graph of the relative error position at different distances between transmitter and receiver which is programmed by the software written in LABVIEW and C++ and the actual position measured by CMM machine. By using the ultrasonic system to evaluate temperature and humidity the error position was improved from 3mm to 0.065mm over 1m by reducing the phase variation.

8 CONCLUSIONS

A new ultrasonic 3D measurement device for use in air has been presented. This system successfully combines both the TOF method and the BFSK method. The technique is based on the multiple-frequency continuous wave (MFcw) with frequency modulation. Three phase shifts between the transmission and reception signal are computed in order to enhance the accuracy of the result. The phase shifts are computed by LABVIEW software and very fast, high resolution DAQ (4MS/S). The environment has been considered as well. The average of relative error position was 23.79 % over 1m. The error of the measured phase shift varied within 1 degree, caused by harmonics-distorted waves due to acoustic cross-coupling between the transducers, change in temperature and change in humidity, even using the ultrasonic system to measure temperature and humidity.

REFERENCES

MARIOLI. D.: IEEE Trans. Meas, **41, 93** (1992).

TARDAJOS. G, GAITANO. G. G and M. F. R.: Rev. Sci. Instrum, **65** (1994).

HUANG. S. S, HUANG. C. F, HUANG. K. N and YOUNG. M. S.: A high accuracy ultrasonic distance measurement system using binary frequency shift-keyed signal and phase detection, **73** (2002), 3671-3677.

YANG. M. H, HUANG. C. F, HUANG. S. S, HUANG. K. N and YOUNG. M. S.: A high accurate ultrasonic measurement system for tremor using binary amplitude-shift-keying and phase-shift method, April **15** (2003), 61-67.

SCHEINZER. H and ELMER. H.: High resolution ultrasonic distance measurement systems using pulse compression and their applications, **295-296** (2005), 301-306.

HUANG. C. F, YANG. M. H and LI. C. Y.: Multiple- frequency continuous wave ultrasonic system for accurate distance measurement, **70** (1998), 1452-1458.

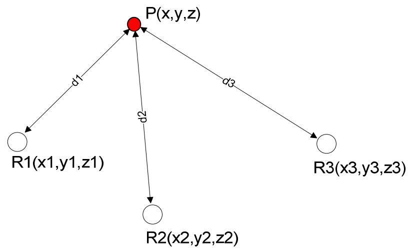

Figure. 1: locations of the position and the receivers

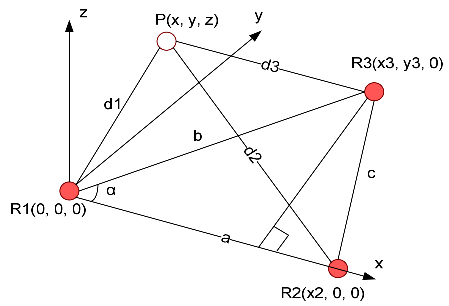

Figure. 2: Positions of the receivers in coordinate system R

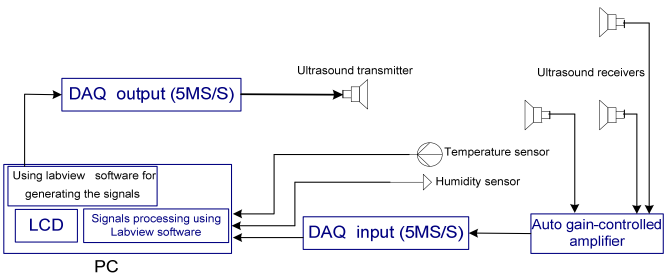

Figure. 3: A block diagram of the system

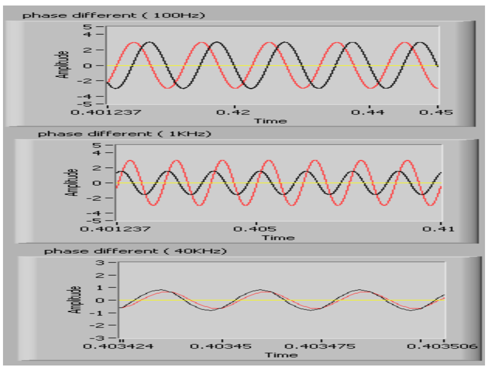

Figure. 4: different phase between transmitter and receiver signal

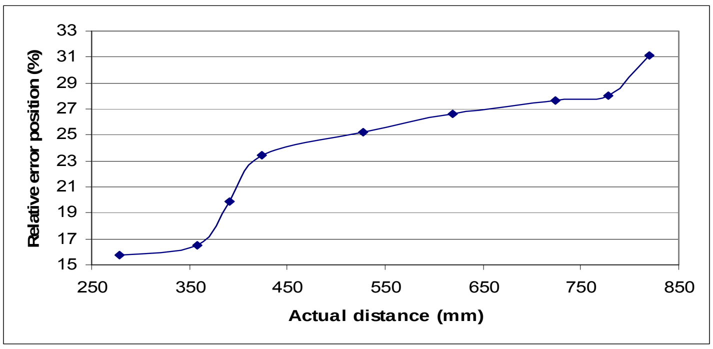

Figure. 5: different phase between transmitter and receiver signal